HHS Public Access

Author manuscript

Biomed Image Registration. Author manuscript; available in PMC 2016 January 06.

Published in final edited form as:

Biomed Image Registration. 2012 ; 7359: 286–295. doi:10.1007/978-3-642-31340-0_30.

Non-Rigid Image Registration Using Gaussian Mixture Models

Sangeetha Somayajula[1,*], **Anand A. Joshi**[2], and **Richard M. Leahy**[2]

[1]Dept. of Informatics IT, Merck Research Laboratories, Boston MA

[2]Signal and Image Processing Institute, University of Southern California, Los Angeles CA

Abstract

Non-rigid mutual information (MI) based image registration is prone to converge to local optima due to Parzen or histogram based density estimation used in conjunction with estimation of a high dimensional deformation field. We describe an approach for non-rigid registration that uses the log-likelihood of the target image given the deformed template as a similarity metric, wherein the distribution is modeled using a Gaussian mixture model (GMM). Using GMMs reduces the density estimation step to that of estimating the parameters of the GMM, thus being more computationally efficient and requiring fewer number of samples for accurate estimation. We compare the performance of our approach (GMM-Cond) with that of MI with Parzen density estimation (Parzen-MI), on inter-subject and inter-modality (CT to MR) mouse images. Mouse image registration is challenging because of the presence of a rigid skeleton within non-rigid soft tissue, and due to major shape and posture variability in inter-subject registration. The results show that GMM-Cond has higher registration accuracy than Parzen-MI in terms of sum of squared difference in intensity and dice coefficients of overall and skeletal overlap. The GMM-Cond approach is a general approach that can be considered a semi-parametric approximation to MI based registration, and can be used an alternative to MI for high dimensional non-rigid registration.

1 Introduction

Longitudinal and inter-subject imaging studies are often performed to study changes in anatomy and function in a subject over a period of time, or across populations. Non-rigid registration is required to normalize anatomical changes such as posture variability in longitudinal studies or anatomical variability across populations in inter-subject studies. Several non-rigid registration algorithms have been developed, a review of which can be found in [7].

Mutual information (MI) measures the amount of information shared between two random variables and can be used as a similarity metric in image registration. It has been successfully applied to multi-modality rigid registration [21] and some approaches to non-rigid registration using MI have also been proposed in [5], [15]. However, MI is a non-convex function of the registration parameters and the registration could converge to an inaccurate local optimum. The problem of converging to local optima is exacerbated in the

[*]Work done while at University of Southern California

non-rigid registration case because of the increased dimensionality of the deformation field compared to the rigid case. Additionally, MI between the reference image (target) and the image to be registered (template) is a function of the joint density of their intensities, which is unknown. Typically a non-parametric approach such as Parzen windowing is used to estimate the entire joint density from the images [14]. This approach requires appropriate choice of the Parzen window width, which is usually taken as a design parameter and kept fixed over the entire sample. This has the drawback that for long-tailed distributions the density estimate tends to be noisy at the tails, and increasing the window width to deal with this might lead to oversmoothing the details in the distribution [4]. The former scenario would result in a cost function that has more local optima, while the latter could lead to inaccurate registration results. The non-parametric approach also requires a large number of samples to accurately estimate the distribution.

Maximizing MI is closely related to maximizing the joint probability of the target and template images, or the conditional probability of the target given the template image [6], [8], [13]. An interpretation of MI as a special case of maximum likelihood estimation is given in [13]. In [6] a maximum *a posteriori* (MAP) framework for non-rigid registration is used wherein a Parzen-like conditional density estimate is computed and used as the likelihood term. In [23] multinomial joint intensity distributions were used in a MAP framework for registration and a relationship with joint entropy was derived for the uniformative prior case. In [8] a registered training set was used to model the joint intensity distribution using Parzen density estimation and Gaussian mixture models (GMMs), and the estimated distribution was used to perform rigid registration of a test set. Approximating the joint density using multiple Gaussians was described in [18] as an approach to increasing the robustness of a joint entropy based regularizer for limited angle transmission tomography image reconstruction.

In this paper we describe an approach for non-rigid registration that uses the log-likelihood of the target image given the deformed template as a similarity metric for non-rigid registration, wherein the distribution is modeled using a GMM. Gaussian distributions are commonly used in image segmentation to represent the distribution of intensities corresponding to a particular tissue type in MR or CT images [2], [12],[16]. In [2], [12] a unified MAP framework was described for brain segmentation, artifact correction, and non-linear registration with spatial prior maps obtained from a probabilistic atlas. We focus on registration and use GMMs to model the joint intensity distribution of the two MR/CT images to be registered, since their distributions are typically characterized by localized blobs. Using GMMs reduces the density estimation step to that of estimating the parameters of the GMM, which consist of the mean, covariance, and weight of each Gaussian. For images that have a few distinct regions of intensity such as mouse CT images, the number of parameters to be estimated is small and can be robustly estimated from fewer samples compared to the non-parametric approach. Our approach of using the log-likelihood of the target given the template in conjunction with a GMM can be viewed as a semi-parametric alternative to MI based registration when dealing with the high dimensional non-rigid registration case.

We compare the performance of our conditional likelihood metric with GMM parameterization, with that of MI with non-parametric density estimation. We will henceforth refer to these methods as the GMM-Cond and the Parzen-MI methods respectively. We evaluate these methods using mouse CT and MR images. Registration of mice and other small animals is challenging because of the presence of rigid skeleton within non-rigid soft tissue. Additionally, inter-subject whole body mouse images may have considerable shape and postural differences. Registration approaches specific to small animal registration were described in [3], [10], [11], [17], [19], and [22]. Specifically, in [17] and [22] MI was used as a similarity metric for intra-modality mouse CT registration. We evaluate the GMM-Cond approach on inter-modality, inter-subject mouse registration.

2 Methods and Results

Let the target and template images be I_1 and I_2, and their intensity at position $\mathbf{x}$ be $i_1(\mathbf{x})$ and $i_2(\mathbf{x})$ respectively. Let the transformation that maps the template to the target be $T(\mathbf{x}) = \mathbf{x} - \mathbf{u}(\mathbf{x})$, where $\mathbf{u}$ is the displacement field. The deformed template is then represented by $I_2^{\mathbf{u}}$, whose intensities are given by $i_2(\mathbf{x}-\mathbf{u}(\mathbf{x}))$. We define the similarity metric $D_{\mathbf{u}}(I_1, I_2)$ between the target and deformed template as the log likelihood of the target given the deformed template. Assuming that the voxel intensities in I_1 and I_2 are independent identically distributed random variables with joint density $p(i_1, i_2)$, the similarity metric is given by,

$$D_{\mathbf{u}}(I_1, I_2) = \log p(I_1 | I_2^{\mathbf{u}}) = \sum_{\mathbf{x}} \log \frac{p(i_1(\mathbf{x}), i_2(\mathbf{x}-\mathbf{u}(\mathbf{x})))}{p(i_2(\mathbf{x}-\mathbf{u}(\mathbf{x})))}. \quad (1)$$

We assume a Gaussian mixture model for the joint density $p(i_1, i_2)$. Let the number of components of the Gaussian mixture model be K, the mixing proportions be π_k, and $g(i_1, i_2 | m_k, \Sigma_k)$ be a Gaussian with mean m_k and covariance Σ_k, where $k = 1, 2, \cdots, K$. Let the unknown deterministic GMM parameters for each component k be represented as $\theta_k = (\pi_k, m_k, \Sigma_k)$, and let $\Theta = [\theta_1, \theta_2, \cdots, \theta_K]$ be the vector of all unknown parameters. Then, the joint density is given by

$$p(i_1, i_2 | \Theta) = \sum_{k=1}^{K} \pi_k g(i_1, i_2 | m_k, \sum\nolimits_k), \quad (2)$$

where $\pi_k > 0$ and $\sum_{k=1}^{K} \pi_k = 1$.

We use the Laplacian of the displacement field as a regularizing term to penalize deformations that are not smooth. We parameterize the displacement field using the discrete cosine transform (DCT) basis. The DCT bases are eigenfunctions of the discrete Laplacian, so using the DCT representation of the displacement field in conjunction with Laplacian regularization simplifies the regularization term to a diagonal matrix [1]. Let $\beta_i(\mathbf{x})$, $i = 1, 2, \cdots, N_b$, represent the DCT coefficients that parameterize the deformation field and let γ_i, $i = 1, 2, \cdots, N_b$ be the corresponding eigen values of the discrete Laplacian matrix $\mathbf{L}$. Then the norm $\|\mathbf{L}\mathbf{u}(\mathbf{x})\|^2 = \sum_{i=1}^{N_b} \gamma_i^2 \beta_i^2$. The objective function is then given by,

$$\max_{\mathbf{u},\Theta}\sum_{\mathbf{x}}\log p(i_1(\mathbf{x})|i_2(\mathbf{x}-\mathbf{u}(\mathbf{x})),\Theta)-\mu\sum_{i=1}^{N_b}{\gamma_i}^2{\beta_i}^2, \quad (3)$$

where μ is a hyperparameter that controls the weight on the regularizing term.

To simplify the problem, we replace the combined optimization with respect to the deformation field and GMM parameters with an iterative two step procedure. Here, the GMM parameters are first estimated from the target and deformed template images through maximum likelihood estimation, and the deformation field is then computed given the estimated GMM parameters. The two step optimization is given by

$$\hat{\Theta}(\hat{\mathbf{u}}^m)=\arg\max_{\Theta}\sum_{\mathbf{x}}\log p(i_1(\mathbf{x}),i_2(\mathbf{x}-\hat{\mathbf{u}}^m(\mathbf{x}))|\Theta) \quad (4)$$

$$\hat{\mathbf{u}}^{m+1}=\arg\max_{\mathbf{u}}\sum_{\mathbf{x}}\log p(i_1(\mathbf{x})|i_2(\mathbf{x}-\mathbf{u}(\mathbf{x})),\hat{\Theta}(\hat{\mathbf{u}}^m))-\mu\sum_{i=1}^{N_b}{\gamma_i}^2{\beta_i}^2, \quad (5)$$

where $\hat{\mathbf{u}}_m$ represents the estimated deformation field at overall optimization iteration m. The estimation of GMM parameters is described in the next section. The estimation of the deformation field in Equation 5 given the GMM parameters is performed using conjugate gradient (CG) optimization with Armijo line search.

2.1 Estimation of parameters of Gaussian mixture model

The maximum likelihood estimate of the GMM parameters $\hat{\Theta}$ in Equation 4 can be obtained by the expectation maximization (EM) algorithm [9]. Let the data sample at voxel j corresponding to the position $\mathbf{x}_j$ be $S_j^{\mathbf{u}}=[i_1(\mathbf{x}_j),i_2(\mathbf{x}_j-\mathbf{u}(\mathbf{x}_j))]^T$, where j = 1, 2, ⋯,N, and N is the number of voxels in each image. The component of the GMM from which S_j arises is taken as the hidden variable in the EM algorithm. The EM update equations are given in Equations 6 – 9.

$$\tau_{jk}^i=\frac{\pi_k^i g(S_j^{\mathbf{u}},m_k^i(\mathbf{u}),\sum_k^i(\mathbf{u}))}{\sum_{h=1}^K\pi_h^i(\mathbf{u})g(S_j^{\mathbf{u}},m_h^i(\mathbf{u}),\sum_h^i(\mathbf{u}))} \quad (6)$$

$$\pi_k^{i+1}(\mathbf{u})=\frac{1}{N}\sum_{j=1}^N\tau_{jk}^i \quad (7)$$

$$m_k^{i+1}(\mathbf{u})=\frac{\sum_{j=1}^N\tau_{jk}^i S_j^{\mathbf{u}}}{\sum_{j=1}^N\tau_{jk}^i} \quad (8)$$

$$\sum_k^{i+1}(\mathbf{u}) = \frac{\sum_{j=1}^{N}\tau_{jk}^{i}(S_j^{\mathbf{u}} - m_k^{i+1}(\mathbf{u}))(S_j^{\mathbf{u}} - m_k^{i+1}(\mathbf{u}))^T}{\sum_{j=1}^{N}\tau_{jk}^{i}}, \quad (9)$$

where $\pi_k^i(\mathbf{u}), m_k^i(\mathbf{u})$, and $\sum_k^i(\mathbf{u})$ are the GMM parameter estimates at EM iteration *i* and deformation field **u**. The objective function to be optimized in Equation 4 is a non-convex function of Θ, so a good initial estimate is needed to converge to a global optimum. We use the k-nearest neighbors algorithm [14] to identify cluster centers in the joint histogram of the target and template images, and the number of samples that fall into a particular cluster. The cluster centers and the proportion of samples in a cluster relative to the total number of samples were used as the initializations m_k^0 and p_k^0 respectively, and $\sum_k^0$ was assumed to be identity for all *k*. The number of clusters was chosen to visually match the initial histogram of the two images. Assuming a reasonable initial global alignment, the number of clusters was then kept constant throughout the registration process.

Figure 1 shows the GMM estimate of the joint pdf of intensities of the target and template images shown in Figure 2 (a) and (b). The joint histogram of the intensities of these two images is shown in Figure 1 (a), and the pdf estimated using GMM is shown in Figure 1 (b) with the component means overlaid. The number of components was chosen to be $K = 7$ to match the joint histogram.

2.2 Relation to Mutual Information

Let the random variables corresponding to the intensities of I_1 and $I_2^{\mathbf{u}}$ be ζ_1 and ζ_2 respectively. Mutual information between ζ_1 and ζ_2 is defined as,

$$D(\zeta_1, \zeta_2) = \int p(z_1, z_2)\log\frac{p(z_1,z_2)}{p(z_1)(z_2)}dz_1dz_2 = E(\log\frac{p(z_1,z_2)}{p(z_1)p(z_2)}). \quad (10)$$

MI between two random variables can be interpreted as the reduction in uncertainty of one random variable given the other. Using MI as a similarity metric for registration aims to find a deformation that makes the joint density of the target and deformed template images maximally clustered, thus implying that the uncertainty of one image given the other is minimized [21].

An alternative formulation can be obtained by approximating the expectation in Equation 10 by a sample mean where the intensity at each voxel in the target and deformed template images constitutes the random sample. Hence we get

$$\begin{aligned}\hat{D}(\zeta_1, \zeta_2) &= \frac{1}{N}\sum_{\mathbf{x}}\log\frac{p(i_1(\mathbf{x}), i_2(\mathbf{x}-\mathbf{u}(\mathbf{x})))}{p(i_1(\mathbf{x}))p(i_2(\mathbf{x}-\mathbf{u}(\mathbf{x})))} \\ &= \frac{1}{N}\sum_{\mathbf{x}}\log\frac{p(i_1(\mathbf{x}), i_2(\mathbf{x}-\mathbf{u}(\mathbf{x})))}{p(i_2(\mathbf{x}-\mathbf{u}(\mathbf{x})))} - \frac{1}{N}\sum_{\mathbf{x}}\log p(i_1(\mathbf{x})).\end{aligned} \quad (11)$$

Since the target is fixed and independent of **u**(**x**), dropping the terms containing the marginal density $p(i_1)$, we get the approximate MI based similarity metric as

$$\hat{D}(\zeta_1, \zeta_2) = \frac{1}{N} \sum_{\mathbf{x}} \log \frac{p(i_1(\mathbf{x}), i_2(\mathbf{x} - \mathbf{u}(\mathbf{x})))}{p(i_2(\mathbf{x} - \mathbf{u}(\mathbf{x})))}. \quad (12)$$

Thus, computing the deformation field that maximizes mutual information is approximately equivalent to maximizing the conditional density of the target given the template image as defined in Equation 1. In [13] a similar relationship between maximum likelihood and conditional entropy was derived. The pdf $p(i_1, i_2)$ in Equation 12 is unknown, and needs to be estimated. The pdf can be estimated using a non-parametric approach such as Parzen windowing or a GMM based approach can be taken to parametrize the pdf and estimate those parameters.

The Parzen window estimate of a pdf at random variable values z_1, z_2 is defined by [14]

$$p(z_1, z_2) = \frac{1}{N} \sum_{j=1}^{N} g\left(\frac{z_1 - i_1(j)}{\sigma}\right) g\left(\frac{z_2 - i_2^{\mathbf{u}}(j)}{\sigma}\right), \quad (13)$$

where $g\left(\frac{z_2}{\sigma}\right)$ is a Gaussian window of width σ, which is usually taken as a design parameter. Note that this can be considered as a Gaussian mixture model with as many Gaussians as the number of samples ($K = N$), with mean given by the sample $m_k = [i_1(k), i_2^{\mathbf{u}}(k)]^T$, fixed standard deviation $\sum_k = \begin{bmatrix} \sigma^2 & 0 \\ 0 & \sigma^2 \end{bmatrix}$, and equal weighting probabilities $\pi_k = \frac{1}{N}$. However, we expect the GMM-Cond approach to have two advantages over the Parzen-MI approach

1. The density estimation requires estimation of 6*K* GMM parameters that can be robustly estimated from the given images for small *K*. In contrast, the Parzen-MI approach computes the entire $N_{bin} \times N_{bin}$ pdf from the samples, where N_{bin} is the number of bins at which the pdf is computed
2. Estimation of the displacement field may be more robust to trapping in local minima because of the much lower dimensionality with which the joint density is parameterized.

We expect to gain computationally as well as in robustness from this reduction in dimensionality of the problem. However, if the joint density does not fit a GMM, the number of mixture components might be large, approaching a Parzen window estimate.

2.3 Results

We perform validation studies of our method using multi-modality (CT and MR) inter-subject mouse images. Mouse CT images typically consist of mainly soft tissue versus bone contrast, and can be assumed to follow a GMM. Though mouse MR images have a larger number of intensity levels than the CT, the number of components required in the GMM is not prohibitively large. We consider two mice that were imaged using both MR and CT (referred to as MR1 and CT1, MR2 and CT2) and two other mice that were imaged using only CT (referred to as CT3 and CT4). This gives 6 possible inter-modality, inter-subject registrations (CT1-MR2, CT3-MR2, CT4-MR2, CT2-MR1,CT3-MR1, CT4-MR1). The MR

images were obtained on a Biospec 7T system at a resolution of 0.23 × 0.17 × 0.50 mm. The CT images corresponding to the MR were acquired on a Siemens Inveon system and the others were obtained from a microCT system, at a resolution of 0.2 × 0.2 × 0.2 mm. We first perform a 12 parameter affine registration of the CT images to the MR image using the AIR software [20]. We downsampled the MR and affinely registered CT images to size 128 × 128 × 64 to reduce computation. The downsampled MR and affinely registered CT images were then used as the target and template images respectively for non rigid registration. We compare our semi-parametric GMM-Cond approach to non-parametric Parzen-MI approach in the context of high-dimensional non-rigid registration, rather than comparing to existing registration algorithms that address mouse registration with application specific constraints such as skeletal rigidity. The goal is to evaluate GMM-Cond as a general framework for non-rigid inter-modality registration in small animal studies.

For both methods, we used 15 × 15 × 15 DCT bases to represent the displacement field. We choose the weight μ on the regularizing term such that the determinant of the Jacobian of the displacement field is positive. For the Parzen-MI registration we followed a hierarchical approach, first aligning the images that were smoothed with a Gaussian of width 3 voxels, and used the displacement field thus obtained to initialize the registration of the original images. We observed that directly aligning the original images causes the algorithm to reach an inaccurate local minimum in a few iterations. A Parzen window width of $\sigma = 5$ was used to compute the distribution at every iteration. For the GMM-Cond approach, we used 5 overall iterations between the density estimation and deformation field estimation. Each displacement field estimation involved 50 iterations of the CG algorithm. Coronal view of the registered images for one dataset along with the target and template images are shown in Figure 2. We used $K = 7$ components in the GMM for this dataset. The outline of the body and lungs of the target image was overlaid in green on all the images. We applied the displacement field resulting from both registration algorithms to the higher resolution images for display purposes. We quantify the performance of the registration through three measures:

1. Overall overlap: The target and template images can be segmented into mouse and background regions. The overall overlap of the target and deformed template can then be measured by computing the dice coefficients of the region labeled as mouse in the two images.
2. Overlap of skeleton: The skeleton can be segmented in the target and template images by thresholding. The dice coefficients of the skeleton in the target and deformed template images give a measure of overlap in the skeleton.
3. Mean squared difference (MSD) between intensities: The target MR image has a corresponding CT image acquired with it. The normalized mean squared difference between intensities of the CT corresponding to the target, and the deformed template images gives a measure of registration accuracy.

The average and standard deviation values of the three measures for the 6 inter-subject CT to MR registrations are given in Table 1.

It can be seen from the images and the outline overlay that the GMM-Cond method shows better overall shape and lung alignment compared to the MI-Parzen and AIR methods. On average, the GMM-Cond method has higher dice coefficients for the skeleton as well as overall shape, and lower normalized MSD between intensities than the MI-Parzen and AIR registration methods, indicating better alignment. It is promising that the GMM-Cond shows improved performance for the inter-subject, multi-modality registration considered, since these images have considerable difference in intensities, overall shape, and skeletal structure.

3 Discussion

We used the conditional density of the target given the deformed template as a similarity metric for non-rigid registration, wherein the conditional density is modeled as a Gaussian mixture model. A DCT representation of the deformation field was used in conjunction with a Laplacian regularizing term to reduce computation. We compared the performance of our approach with that of Parzen-MI based approach using multimodality MR/CT mouse images.

The GMM-Cond approach showed higher registration accuracy than the Parzen-MI approach in terms of dice coefficients and mean squared difference between intensities of the target and registered images. The GMM parametrization is not only computationally more efficient than the Parzen method, but also improves performance by reducing the overall dimensionality of the estimation problem, and through more robust and accurate density estimation. Additionally, the only design parameter that needs to be chosen is the number of clusters in the GMM, which can be obtained from the initial joint histogram.

The performance of the GMM-Cond method is promising as it performs better than the Parzen MI approach for multi-modality whole body images with postural variations. This indicates that this is a robust approach that can potentially be applied to multimodality non-rigid registration problems. It can be used as an alternative to MI based registration when dealing with high dimensional deformation fields. The GMM-Cond approach can be viewed as a general framework that can be used in conjunction with other models for the deformation field, and with additional constraints specific to the application (e.g., rigidity constraints for the skeleton in mouse images). It should be noted however, that if the joint density of the images does not follow a GMM, a large number of clusters would be required to fit the data, thus increasing the number of parameters to be estimated and might not perform better than Parzen-MI in that case. We expect this approach to be particularly useful in applications where the images have a few distinct regions of intensity such as mouse CT images.

Acknowledgments

This work was supported by grants NIH/NIBIB P41 EB015922, P41 RR013642 and R01 NS074980

References

1. Ashburner J, Friston K. Nonlinear spatial normalization using basis functions. Human Brain Mapping. 1999; 7(4):254–266. [PubMed: 10408769]

2. Ashburner J, Friston KJ. Unified segmentation. NeuroImage. 2005; 26(3):839–851. [PubMed: 15955494]
3. Baiker, M.; Staring, M.; Lwik, C.; Reiber, J.; Lelieveldt, B. Automated registration of whole-body follow-up microct data of mice. In: Fichtinger, G.; Martel, A.; Peters, T., editors. Medical Image Computing and Computer-Assisted Intervention MICCAI 2011. Springer; Berlin / Heidelberg: p. 516-523.Lecture Notes in Computer Science
4. Silverman, BW. Density estimation for Statistics and Data analysis. Chapman and Hall; 1986.
5. D'Agostino E, Maes F, Vandermeulen D, Suetens P. A viscous fluid model for multimodal non-rigid image registration using mutual information. Medical Image Analysis. 2003; 7(4):565–575. [PubMed: 14561559]
6. Zhang J, Rangarajan A. Bayesian multimodality non-rigid image registration via conditional density estimation. Information Proc in Med Imaging. 2003:499–511.
7. Krum W, Griffin LD, Hill DLG. Non-rigid image registration: Theory and practice. Br Journ Radiol. 2004; 1(77):S140–S153.
8. Leventon, M.; Grimson, W. Multi-modal volume registration using joint intensity distributions. In: Wells, W.; Colchester, A.; Delp, S., editors. Medical Image Computing and Computer-Assisted Intervention MICCAI98, Lecture Notes in Computer Science. Vol. 1496. Springer; Berlin / Heidelberg: 1998. p. 1057-1066.
9. MacLachlan, G.; Peel, D. Finite Mixture Models. Wiley; 2000.
10. Kovacevic N, Hamameh G, Henkelman M. Anatomically guided registration of whole body mouse MR images. MICCAI. 2003:870–877.
11. Papademetris X, Dione DP, Dobrucki LW, Staib LH, Sinusas AJ. Articulated rigid registration for serial lower-limb mouse imaging. MICCAI. 2005; (2):919–926. [PubMed: 16686048]
12. Pohl KM, Fisher J, Grimson WEL, Kikinis R, Wells WM. A bayesian model for joint segmentation and registration. NeuroImage. 2006; 31(1):228–239. [PubMed: 16466677]
13. Roche, A.; Mal, G.; Ayache, N.; Prima, S. MICCAI. Springer-Verlag; 1999. Towards a better comprehension of similarity measures used in medical image registration; p. 555-566.
14. Duda, RO.; Hart, PE.; Stork, DG. Pattern Classification. 2. Wiley; 2001.
15. Rueckert D, Sonoda LI, Hayes C, Hill DL, Leach MO, Hawkes DJ. Nonrigid registration using free-form deformations: application to breast mr images. IEEE Trans Med Imaging. 1999; 18(8): 712–721. [PubMed: 10534053]
16. Shattuck DW, Sandor-Leahy SR, Schaper KA, Rottenberg DA, Leahy RM. Magnetic resonance image tissue classification using a partial volume model. NeuroImage. 2001; 13(5):856–876. [PubMed: 11304082]
17. Somayajula, S.; Joshi, A.; Leahy, R. Mutual information based non-rigid mouse registration using a scale-space approach. 5th IEEE Intl. Symposium on Biomedical Imaging; 2008. p. 1147-1150.
18. de Sompel DV, Brady M. Regularising limited view tomography using anatomical reference images and information theoretic similarity metrics. Medical Image Analysis. 2012; 16(1):278–300. [PubMed: 21962917]
19. Wang H, Stout D, Chatziioannou A. Estimation of mouse organ locations through registration of a statistical mouse atlas with micro-ct images. Medical Imaging, IEEE Transactions on. 2012; 31(1): 88–102.
20. Woods R, Grafton S, Watson J, Sicotte N, Mazziotta J. Automated image registration: I. General methods and intrasubject, intramodality validation. Journal of Computed Assisted Tomography. 1998; 22:139–152.
21. Wells W, Viola P, Atsumi H, Nakajima S, Nakajima S, Kikinis R. Multimodal volume registration by maximization of mutual information. Med Image Analysis. 1996; 1(1):35–51.
22. Li X, Peterson TE, Gore JC, Dawant BM. Automatic inter-subject registration of whole body images. Lecture Notes in Computer Science. 2006; 4057:18–25.
23. Zöllei, L.; Jenkinson, M.; Timoner, S.; Wells, W. A marginalized map approach and em optimization for pair-wise registration; Inf processing in medical imaging; 2007. p. 662-674.

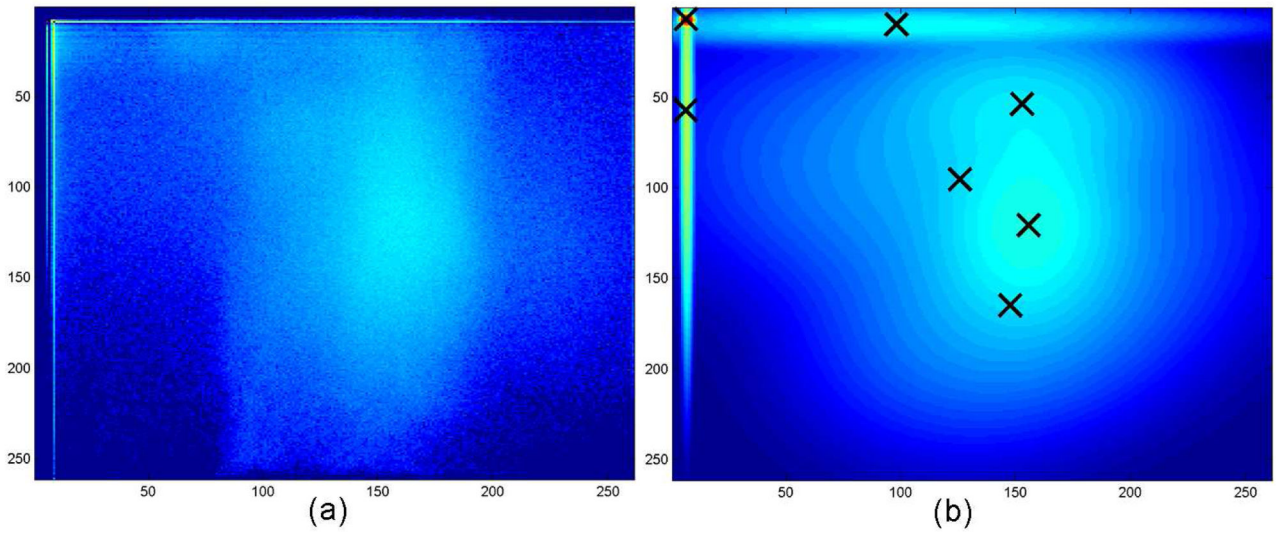

Fig. 1.

Estimation of joint pdf of images in Fig. 2 (a) and (b) : (a) Joint histogram of images, (b) GMM estimate (the component means shown with 'x' marks).

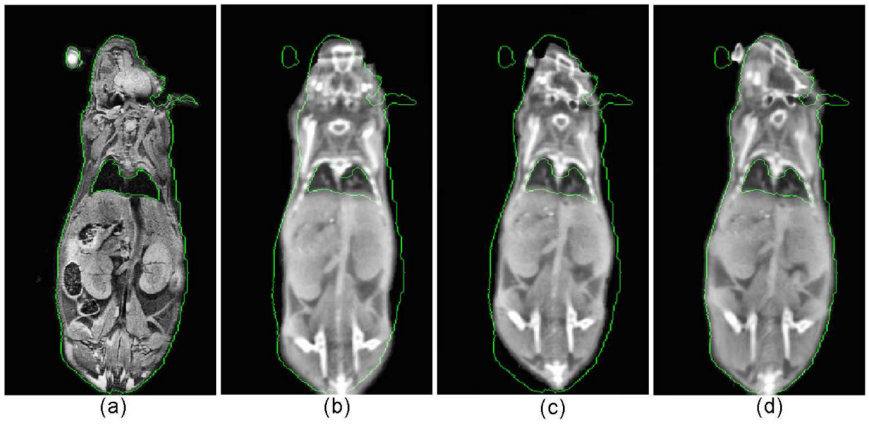

Fig. 2.

Multi-modality inter-subject registration: Coronal view of (a) target MR image with outline of body and lungs, (b) template CT image affinely registered to MR, (c) Parzen-MI registered image, and (d) GMM-Cond registered image. Images (b)–(d) are shown with target body and lung outlines.

Table 1

Quantitative measures of overlap

Mean ± SD of dice coefficients for overall overlap		
Affine	**Parzen-MI**	**GMM-Cond**
0.84 ± 0.03	**0.87** ± 0.04	**0.91** ± 0.03
Mean ± SD of dice coefficients for overlap of skeleton		
0.24 ± 0.07	**0.31** ± 0.07	**0.34** ± 0.04
Mean ± SD of squared difference between intensities		
0.56 ± 0.07	**0.50** ± 0.07	**0.44** ± 0.11